

Red giant seismology: observations

Benoît Mosser^{1,a}

LESIA, CNRS, Université Pierre et Marie Curie, Université Denis Diderot, Observatoire de Paris,
92195 Meudon cedex, France

Abstract. The CoRoT and Kepler missions provide us with thousands of red-giant light curves that allow a very precise asteroseismic study of these objects. Before CoRoT and Kepler, the red-giant oscillation patterns remained obscure. Now, these spectra are much more clear and unveil many crucial interior structure properties. For thousands of red giants, we can derive from the seismic data precise estimates of the stellar mass and radius, the evolutionary status of the giants (with a clear difference between clump and RGB stars), the internal differential rotation, the mass loss, the distance of the stars... Analysing this mass of information is made easy by the identification of the largely homologous red-giant oscillation patterns. For the first time, both pressure and mixed mode oscillation patterns can be precisely depicted. The mixed-mode analysis allows us, for instance, to probe directly the stellar core. Fine details completing the red-giant oscillation pattern then provide further information for a more detailed view on the interior structure, including differential rotation.

1 Introduction

The CNES CoRoT mission (Michel et al., 2008) and the NASA *Kepler* mission (Borucki et al., 2010) have opened a new era in red giant asteroseismology (De Ridder et al., 2009), with thousands of high-precision photometric light curves. This amount of data has motivated collaborative working in dedicated working groups, in an organisation very profitable for promoting efficient work and impressive results (e.g. Hekker et al., 2009; Bedding et al., 2010; Huber et al., 2010; Mosser et al., 2010). This paper has benefitted from all this work.

Before space-borne observation, ground-based observations have revealed that red giants, with an outer convective envelope, show solar-like oscillations (e.g. Frandsen et al., 2002). Owing to their low gravity, oscillations in red giants are excited at low frequency. Owing to their low mean density, their oscillation pattern show frequency differences at low frequency, with the so-called large separation of the order of a few microhertz. Limitations due to both too short observing runs (even if the longest lasted about two months) and a poor duty cycle have hampered a rich output of these ground-based observations but raised crucial questions concerning the degree of the observed modes and the mode lifetimes. Frandsen et al. (2002) explicitly state that “a most important and exciting result of [their] study is the confirmation of the possibility, suggested by the results reported on α UMa and Arcturus, to observe solar-like oscillations in stars on the red giant branch”. These questions were not answered by observations with the microsatellite MOST (e.g. Barban et al., 2007), with time series limited to one month. However, the pioneering role of these observations was highly valuable, so that red giants were considered as valuable asteroseismic targets. Without them, both CoRoT and *Kepler* should have missed an impressive harvest.

In Section 2, we first present results obtained when considering global seismic parameters only. Such parameters allow us to perform ensemble asteroseismology. The tools for identifying the individual frequencies are then presented in Section 3. The identification of the dipole mixed-mode pattern,

^a e-mail: benoit.mosser@obspm.fr

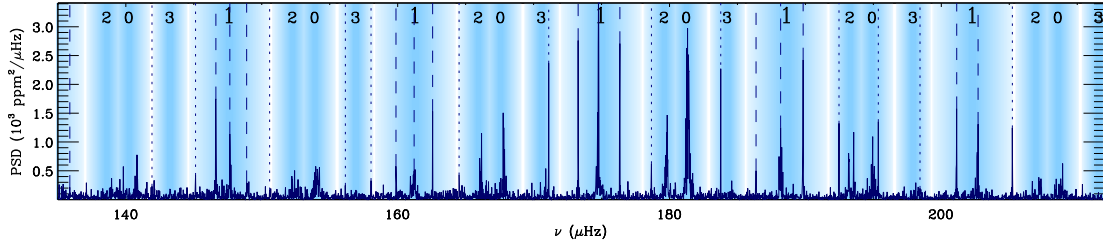


Fig. 1. Power density spectrum of the star KIC 9882316, with superimposed mode identification provided by the red giant oscillation universal pattern. Dashed and dotted lines indicate the position of the peaks identified as dipole mixed modes. Pressure dominated dipole modes are located close to the positions marked by 1.

not as easily identifiable as the radial pressure mode pattern, is developed in Section 4. These mixed modes unveil unique properties of the core. Open questions and upcoming work are presented in Section 5.

An introduction to red giant seismology, by Christensen-Dalsgaard (2011) and Montalbán et al. (2012) for theoretical aspects or by Bedding (2011) in an observational perspective, can be useful for setting the scene.

2 Scaling relations

A large amount of scaling relations have been recently derived in asteroseismology (e.g. Hekker et al., 2009; Kallinger et al., 2010; Huber et al., 2011). Such relations are based on global seismic parameters used to sum up the mean properties of a solar-like oscillation spectrum. They allow us to perform ensemble asteroseismology, since they monitor the evolution of various parameters for a large population of stars.

2.1 Global seismic parameters

Most scaling relations involve the large separation $\Delta\nu$ and/or the frequency ν_{\max} corresponding to the maximum oscillation signal. The determination of these global seismic parameters can be done diversely (e.g. Hekker et al., 2011).

Here, we use essentially the data analysis provided by the method of Mosser & Appourchaux (2009), called envelope autocorrelation function (EACF). Deriving the large separation from the autocorrelation of the time series is physically efficient, since it corresponds to measure the delay between any oscillation signal first seen directly, then after propagation throughout the stellar diameter back and forth. Achieving this autocorrelation of the time series of the oscillation signal by computing the Fourier transform of its Fourier transform of the oscillation signal is computationally very efficient. Considering a windowing of the spectrum, as proposed by Roxburgh (2009), allows us to select a given frequency range, or to investigate the variation of the frequency separations with frequency, or to study independently the frequency separations of the even and odd ridge (Mosser, 2010). With a filter width corresponding to the frequency range around ν_{\max} where solar-like oscillations are excited, the method provides the mean value of the observed large separation. Last but not least, the methodology used by the EACF method provides a test for determining the reliability of the detection, based on the H0 hypothesis.

Scaling relation in asteroseismology is an old story, when Eddington (1917) noted that the pulsation of cepheids are related to their mean density. This can be expressed by the scaling relation

$$\Delta\nu \propto \sqrt{\frac{M}{R^3}} \quad (1)$$

where $\Delta\nu$ is the mean large separation, and M and R are the stellar mass and radius. $\Delta\nu$ is usually defined as the mean frequency difference between consecutive radial modes (Fig. 1). In fact, this definition is misleading: frequency differences yield the *observed value* of the large separation, which is different from the *asymptotic value* that verifies Eq. (1). The link between the large separation and the mean stellar density has been addressed by White et al. (2011) for different stellar masses and evolutionary stages. The relation between the observed and asymptotic values of the large separation is established by Mosser et al. (2013):

$$\Delta\nu_{\text{as}} = (1 + \zeta) \Delta\nu_{\text{obs}}, \quad (2)$$

with

$$\zeta = \frac{0.57}{n_{\text{max}}} \quad (\text{main-sequence regime: } n_{\text{max}} \geq 15), \quad (3)$$

$$\zeta = 0.038 \quad (\text{red giant regime: } n_{\text{max}} \leq 15), \quad (4)$$

where $n_{\text{max}} = \nu_{\text{max}}/\Delta\nu$ measures the frequency of maximum of oscillation signal in a dimensionless manner. The relation between ν_{max} and the acoustic cutoff frequency ν_c proposed by Belkacem et al. (2011) introduces the Mach number \mathcal{M} in the uppermost convective layers so that $\nu_{\text{max}} \propto \nu_c \mathcal{M}^3$. The variation of this number with stellar type and evolution is limited but remains unknown.

2.2 Seismic mass and radius

The importance of the measurements of $\Delta\nu$ and ν_{max} is emphasized by their ability to provide relevant estimates of the stellar mass and radius

$$\frac{R_{\text{seis}}}{R_{\odot}} = \left(\frac{\nu_{\text{max}}}{\nu_{\text{ref}}} \right) \left(\frac{\Delta\nu_{\text{as}}}{\Delta\nu_{\text{ref}}} \right)^{-2} \left(\frac{T_{\text{eff}}}{T_{\odot}} \right)^{1/2}, \quad (5)$$

$$\frac{M_{\text{seis}}}{M_{\odot}} = \left(\frac{\nu_{\text{max}}}{\nu_{\text{ref}}} \right)^3 \left(\frac{\Delta\nu_{\text{as}}}{\Delta\nu_{\text{ref}}} \right)^{-4} \left(\frac{T_{\text{eff}}}{T_{\odot}} \right)^{3/2}. \quad (6)$$

The reference value $\Delta\nu_{\text{ref}} \simeq 3106 \mu\text{Hz}$ and $\nu_{\text{ref}} \simeq 138.8 \mu\text{Hz}$ have been determined by Mosser et al. (2013), relying on the exact use of the second-order asymptotic expression and on the calibration with modeled stars. Unbiased estimated of R and M are provided only if the asymptotic value of the large separation is used. The use of the observed large separation induces significant bias, of the order of 3 % for the radius and 6 % for the mass.

Even if the calibration effort is not complete, the scaling relation give relevant estimates. Mosser et al. (2013) have shown that the correct use of the scaling relations with the asymptotic large separation provides estimates of R and M with uncertainties of about 4 and 8 %, respectively, for low-mass stars. Uncertainties are twice larger when $M \geq 1.3 M_{\odot}$ or for red giants.

2.3 Ensemble asteroseismology

Scaling relations on global parameters allow us to perform ensemble asteroseismology.

- The radius-mass diagram puts in evidence the mass-loss occurring at the tip of the red giant branch (RGB, Fig. 2). The mass loss of low-mass stars is enough for reducing the mass of their envelope to less than $0.2 M_{\odot}$.
- Mathur et al. (2011) have performed a comparative study of the granulation background in giants. The parameters of the background in the Fourier spectrum are closely related to the parameters of the solar-like oscillation, so that a mechanism able to partition the convective energy between oscillation and granulation must exist. For instance Mosser et al. (2012a) have shown that the height-to-background ratio at ν_{max} is constant for red giants, with only a slight difference between RGB and clump stars.

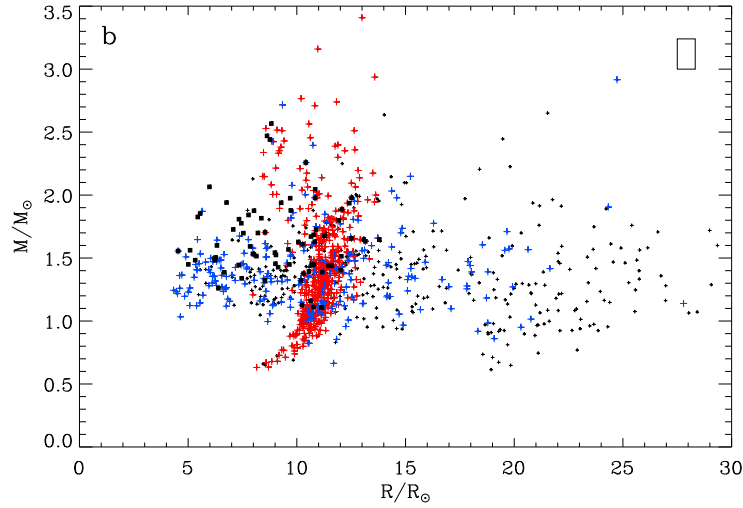


Fig. 2. Asteroseismic mass as a function of the asteroseismic radius. The color code indicates the evolutionary status; clump stars in red, giant branch stars in blue, unknown status in dark grey. The population of giants with low $\ell = 1$ amplitude is indicated with black squares. The rectangles in the upper right corners indicate the mean value of the $1\text{-}\sigma$ error bars. From Mosser et al. (2012a).

- Scaling relations of the oscillation amplitude were reported by different groups (e.g. Mosser et al., 2010, for CoRoT observations), from main-sequence stars to red giants (Huber et al., 2011) or using red giants in clusters (Stello et al., 2011). Previous models have failed for reproducing the scaling relations. With 3D hydrodynamical models representative of the upper layers of sub- and red giant stars, the acoustic mode energy supply rate computed by Samadi et al. (2012) shows that scaling relations of mode amplitudes cannot be extended from main-sequence to red giants because non-adiabatic effects for red giant stars cannot be neglected.

3 Frequency pattern

Any person involved in the data analysis of red giants rapidly gets the impression that all red giant spectra are very similar. This has to be related to the fact that red giants have necessarily very similar interiors. Before evolving into a red giant, the star has undergone the exhaustion of hydrogen in its core, the contraction of its helium core, the separation of the continuously contracting core from the continuously growing envelope, with a thin hydrogen-burning shell at the interface, and the growth of a large convective envelope. All these steps, mostly governed by the properties of the hydrogen-burning shell (equation of state, power supply rate), have erased most of the original characteristics of the stars. After the tip of the RGB, all low-mass red giants pass through the helium flash. As a consequence, they gain a new opportunity to reach almost the same interior structure, as shown by the mass-radius relation of clump stars (Fig. 2).

Mosser et al. (2011b) have capitalized this necessary similarity to set up a method for measuring very precisely the large separation and for identifying in an automated way red-giant oscillation spectra. Assuming that these oscillations obey to a universal pattern, they have proposed that the offset ε of the asymptotic relation (Tassoul, 1980) is a function of the large separation. They have expressed the second-order term of the asymptotic relation with a quadratic term that relates the curvature of the ridges observed in the échelle diagrams:

$$\nu_{n,\ell} = \left[n + \frac{\ell}{2} + \varepsilon(\Delta\nu_{\text{obs}}) - d_{0\ell}(\Delta\nu_{\text{obs}}) + \frac{\alpha_\ell}{2}(n - n_{\text{max}})^2 \right] \Delta\nu_{\text{obs}} \quad (7)$$

We use here the subscript *obs* to emphasize the difference with the asymptotic value. The different $d_{0\ell}$ terms indicate the small spacings of non-radial modes (Mosser et al., 2011b). Mosser et al. (2012b)

have shown that α_0 is also function of the large separation. This implies that all curvatures α_ℓ depend on $\Delta\nu_{\text{obs}}$. This method has proven to be efficient for all red giants, with a large separation in the range $[0.4 - 40 \mu\text{Hz}]$, especially for oscillation spectra recorded with a low signal-to-noise ratio.

The univocal relation between ε_{obs} and $\Delta\nu_{\text{obs}}$, updated by Corsaro et al. (2012), is insured if the large separation is observed in a large frequency range. When determined in a limited frequency range, the small difference of the offset ε between RGB and clump stars allows us to determine the evolutionary status of the giant (Kallinger et al., 2012).

Mosser et al. (2013) have recently shown that the relation $\varepsilon(\Delta\nu_{\text{obs}})$ is an artefact, so that the radial modes of red giants follow the pattern:

$$\nu_{n,0} = \left(n + \frac{1}{4} + 0.037 \frac{n_{\text{max}}^2}{n} \right) \Delta\nu_{\text{as}} = \left(n + \frac{1}{4} + \frac{18.3}{n} \left(\frac{M}{M_\odot} \frac{R_\odot}{R} \frac{T_\odot}{T_{\text{eff}}} \right) \right) \Delta\nu_{\text{as}}. \quad (8)$$

based on the asymptotic value $\Delta\nu_{\text{as}}$ of the large separation. This equation is fully equivalent to Eq. 7, with the relation between the asymptotic and observed values of the large separation provided by Eq. 2.

Departures to such a regular spectrum are due to rapid structure discontinuities. They induce so-called glitches in the oscillation spectrum, as due to the second ionisation of helium (Miglio et al., 2010). Provost et al. (1993) have shown that an asymptotic development can be used for addressing the signature of such discontinuity. However, the red giant oscillation spectrum is also much more complex, due to the presence of other oscillation modes than pure pressure modes.

4 Mixed modes and stellar evolution

4.1 Stellar evolution

Beck et al. (2011) have identified mixed modes in an RGB star. Such mixed modes result from pressure waves propagating in the envelope coupled with gravity waves trapped in the core. Due to the contraction of the inert helium core, the Brunt-Väisälä frequency reaches much higher values than in main-sequence stars, so that the coupling between the different waves in the envelope and in the core is efficient (e.g. Montalbán et al., 2012). This coupling permits the information of gravity modes to percolate to the surface. Hence, Bedding et al. (2011) could show that the mixed-mode frequency separation depends on the evolutionary status of the star and allows us to distinguish helium-burning stars in the red clump from shell hydrogen-burning stars in the RGB. Mosser et al. (2011a) have proposed an alternative method, based on the EACF with narrow filters centered on the dipole modes. These first approaches only deliver the bumped period spacing, significantly perturbed by the coupling of the pressure and gravity waves and quite different from the period spacing $\Delta\Pi_1$ of gravity modes.

4.2 Asymptotic development of the mixed mode pattern

Measuring the period spacing $\Delta\Pi_1$ is derived from the asymptotic development for mixed modes exposed by Mosser et al. (2012c), based on the method exposed by Unno et al. (1989). Observations of red giant with a large number of dipole mixed modes give rise to this development. The mixed-mode frequencies related to the pure pressure dipole mode of radial order n are solutions of the implicit equation:

$$\nu = \nu_{n,\ell=1} + \frac{\Delta\nu}{\pi} \arctan \left[q \tan \pi \left(\frac{1}{\Delta\Pi_1 \nu} - \varepsilon_g \right) \right]. \quad (9)$$

where $\nu_{n,\ell=1}$ is the pure pressure mode frequency previously determined, q is a dimensionless coupling factor, $\Delta\Pi_1$ is the period spacing of pure gravity modes and ε_g is a constant fixed to 0. For each pressure radial order n , one obtains $N+1$ solutions, with $N \simeq \Delta\nu \Delta\Pi_1^{-1} \nu_{\text{max}}^{-2}$. The value of $\Delta\Pi_1$ is derived from a least-squares fit of the observed values to the asymptotic solution. As shown by Mosser et al. (2012c), the observation of high gravity mode orders insures a precise description of the mixed-mode pattern

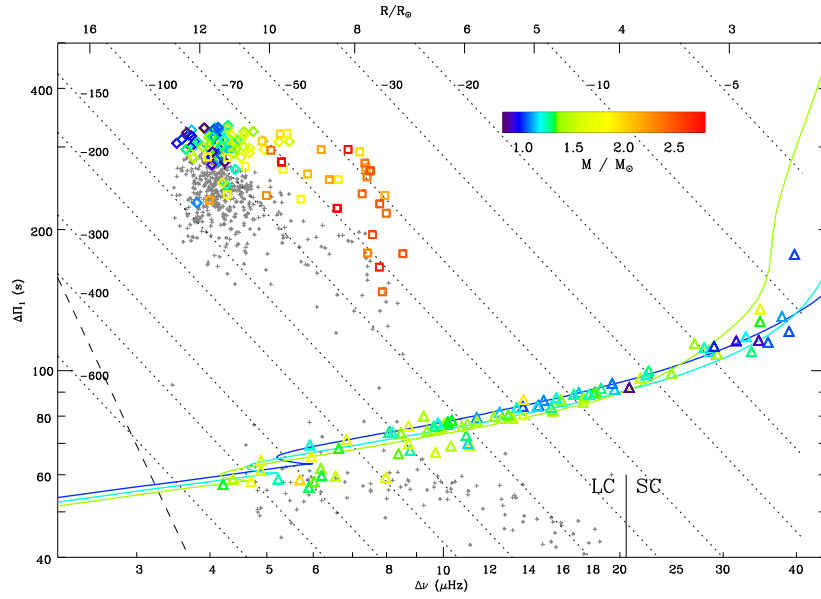


Fig. 3. Gravity-mode period spacing $\Delta\Pi_1$ as a function of the pressure-mode large frequency spacing $\Delta\nu$. Long-cadence data (LC) have $\Delta\nu \leq 20.4 \mu\text{Hz}$. RGB stars are indicated by triangles; clump stars by diamonds; secondary clump stars by squares. Uncertainties in both parameters are smaller than the symbol size. The seismic estimate of the mass is given by the color code. Small gray crosses indicate the bumped periods ΔP_{obs} measured by Mosser et al. (2011a). Dotted lines are n_g isolines. The dashed line in the lower left corner indicates the formal frequency resolution limit. The upper x-axis gives an estimate of the stellar radius for a star whose ν_{max} is related to $\Delta\nu$ according to the mean scaling relation $\nu_{\text{max}} = (\Delta\nu/0.28)^{1.33}$ (both frequencies in μHz). The solid colored lines correspond to a grid of stellar models with masses of 1, 1.2 and $1.4 M_{\odot}$, from the ZAMS to the tip of the RGB. From Mosser et al. (2012c).

with the asymptotic development. As a result, the period $\Delta\Pi_1$ can be determined with a high accuracy (Fig. 3). This is highly valuable for directly characterizing the stellar cores (Montalbán et al., 2012).

For low-mass stars on the RGB, the close relationship between the large separation $\Delta\nu$ and the period spacing $\Delta\Pi_1$ emphasizes the homology of red giants (Fig. 3). This underlines the fact that the properties of the stellar envelope are completely governed by the properties of the helium core and its hydrogen-burning shell.

4.3 Rotational splittings

Beck et al. (2012) have shown that gravity-dominated mixed modes revealed the core rotation in red giant. They analysed the rotational splittings of three red giant oscillation spectra, in the early stages of the RGB. These splittings reveal a significant differential rotation, with a core rotating at least ten times faster than the surface.

Mosser et al. (2012b) have developed a method for analysing rotation splittings in an automated way, based on the EACF function with ultra-narrow filters. This method has provided splittings in more than 260 red giants observed with *Kepler*. A direct identification of the rotational splittings, provided by the method proposed by Mosser et al. (2012c), was also used for more than 100 red giants (Fig. 4, 5). Under the hypothesis that a linear analysis can provide the mean core rotation from the rotational splittings of the gravity-dominated mixed modes, the evolution of this mean core rotation indicates a significant spin down of the core rotation occurs in red giants. This spin down, observed on the RGB but much more marked for clump stars, requires an significant angular momentum transport between the different regions of the star.

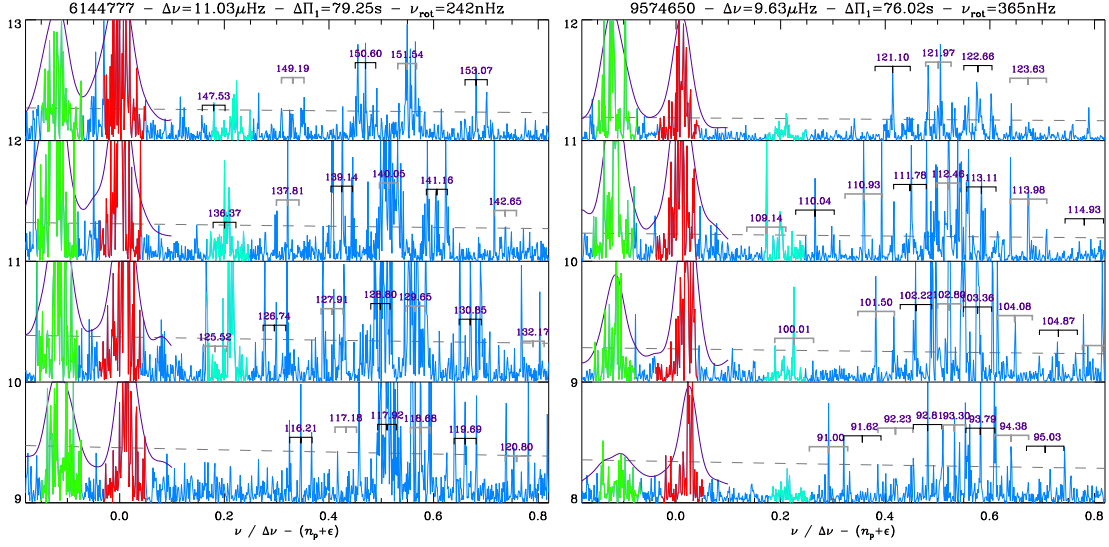


Fig. 4. Zoom on the rotational splittings of the mixed modes in the giants KIC 6144777 and 9574650, in an échelle diagram as a function of the reduced frequency $\nu/\Delta\nu - (n + \varepsilon)$. At low frequency, multiplets are overlapping. Radial and quadrupole modes, in red and green respectively, are located around the dimensionless abscissae 0 and -0.12 . The dashed lines indicates the mean value of the background multiplied by 8. From Mosser et al. (2012b).

Table 1. Asymptotic fit

Modes	Method	Parameters		Remark
		First step	Refined step	
Pressure modes	Universal pattern	Large separation $\Delta\nu$		$\varepsilon = \varepsilon(\Delta\nu)$
			Glitch $\delta\varepsilon$	$d_{01} = d_{01}(\Delta\nu)$ $ \delta\varepsilon \leq 0.02$
Mixed modes	Asymptotic	Period spacing $\Delta\Pi_1$		$\varepsilon_g = 0$
		Coupling factor q		
Rotational splittings	Empirical	Core splittings $\delta\nu_{\text{rot}}$	$\varepsilon_g \neq 0$	
			2 parameters	

5 From asteroseismic observations to stellar physics

The analysis of the thousands of red giant oscillation spectra has just started. The description of these spectra with the combination of the universal red giant oscillation pattern, the asymptotic development of mixed modes and an empirical description of the rotational splittings has proven to be fruitful. As shown by Table 1, four parameters are enough to identify all modes. Refined fits are obtained with eight free parameters, to be compared to the number of fitted modes (in the range 40 - 140) and to the complexity of some spectra (Fig. 5).

Undoubtedly, the high-quality asteroseismic constrains, especially those sounding the stellar core, is promoting large progress in stellar physics.

5.1 Standard candles

The precise asteroseismic constraints on red giants, and especially the precise estimate of the radius from scaling relations, completed with the more precise determination derived from stellar modeling, allows us to use red giants as standard candles (Miglio et al., 2009, 2012). According to Eq. (5), this requires the use of reliable effective temperatures T_{eff} , determined from photometry and colour- T_{eff}

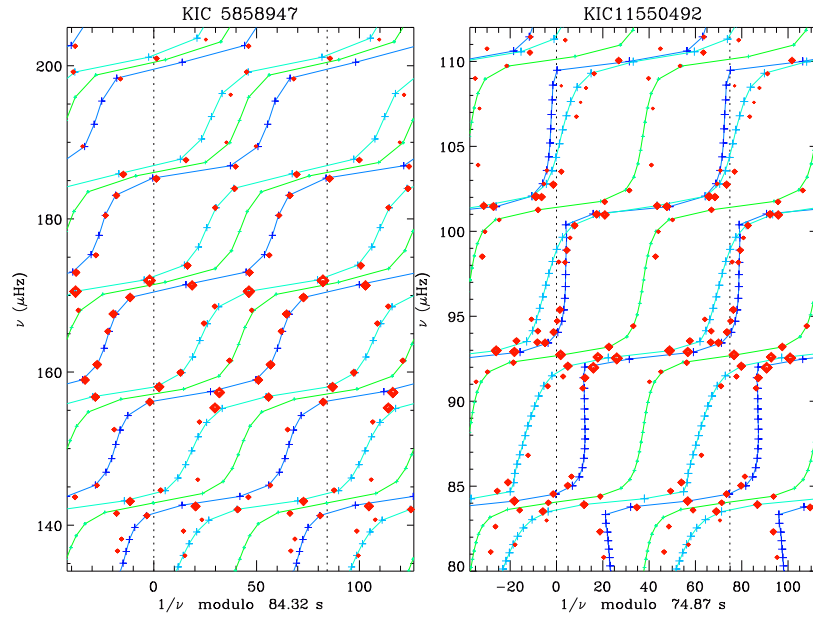


Fig. 5. Gravity échelle diagrams of the two RGB stars KIC 5858947 and 11550492. The x-axis is the period $1/\nu$ modulo the gravity spacing $\Delta\Pi_1$; for clarity, the range has been extended from -0.5 to $1.5 \Delta\Pi_1$. The size of the selected observed mixed modes (red diamonds) indicates their height. Plusses give the expected location of the mixed modes, with $m = -1$ in light blue, $m = 0$ in green and $m = +1$ in dark blue.

calibrations. Luminosities and distances are derived from dereddened apparent 2MASS magnitudes and bolometric corrections. Combining distances with spectroscopic constraints and asteroseismic estimates of the mass allows a detailed characterisation of populations of giants in different regions of the Galaxy observed by *Kepler* and CoRoT at large set of galactic latitudes and longitudes (Miglio et al., 2009, 2012). This topic is more precisely developed by Miglio & al. (2013) in these proceedings.

5.2 Modeling

Modeling effort has been achieved for a limited number of red giants with seismic constraints (Carrier et al., 2010; Miglio et al., 2010; Jiang et al., 2011; di Mauro et al., 2011; Baudin et al., 2012). If not based on grid computing, this effort is time consuming, as it allows to address the physical input in the modeling. Then, it makes the best of the seismic constraints. In some stars, the lifetimes of the gravity-dominated mixed modes is so long that it yet exceeds the total duration of the observation run (31 months at the time this article is written), so that the accuracy of the frequency determination is equal to the frequency resolution (≈ 12 nHz), much better than the current performance of modeling (di Mauro & al., 2013). As a consequence, future developments are very promising.

5.3 Low-amplitude dipole mixed modes

Most red giants spectra show a complex spectrum, with short-lived pressure-dominated and long-lived gravity-dominated mixed modes. A family of red giants shows non-standard spectra, with depressed dipole modes (Mosser et al., 2012a). Such red giants are found at all evolutionary stage from the early RGB to the red clump (Fig. 6). The coupling between the two cavities in the envelope and in the core certainly obeys to specific conditions that govern such a behaviour. Clarifying the situation of these stars will greatly help our understanding of the mixed modes in red giants.

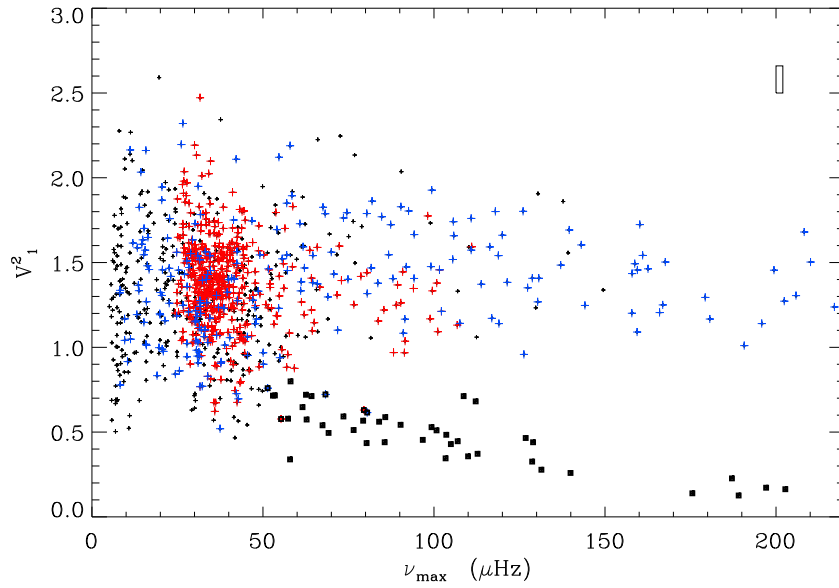


Fig. 6. Visibility V_1^2 as a function of ν_{\max} , with the same color code as in Fig. 2. Large black symbols indicate the population of stars with very low V_1^2 values.

5.4 Upper red giant branch; asymptotic giant branch

Red giants ascending the RGB or the AGB have such large radii that their oscillation occur at very low frequencies, as shown by the analysis of the upper RGB from OGLE observations (Dziembowski & Soszyński, 2010). By extrapolation of the current results, the extension of the *Kepler* mission can provide us with the observation of giants with large separation as low as $0.20 \mu\text{Hz}$. If the scaling relations are still valid, this corresponds to radii of about $80 R_{\odot}$, maybe not enough for investigating the tip of the RGB at all masses, but useful for combining with OGLE results.

5.5 Differential rotation and angular momentum transport

The observation of the rotational splittings implies that angular momentum is, as expected, significantly redistributed between the different regions of the stars. A thorough analysis of this redistribution has just started. This will take time, but we are confident that the new constraints provided by asteroseismic observation will be translated by theoreticians into highly valuable information.

References

- Barban, C., Matthews, J. M., De Ridder, J., et al. 2007, A&A, 468, 1033
- Baudin, F., Barban, C., Goupil, M. J., et al. 2012, A&A, 538, A73
- Beck, P. G., Bedding, T. R., Mosser, B., et al. 2011, Science, 332, 205
- Beck, P. G., Montalbán, J., Kallinger, T., et al. 2012, Nature, 481, 55
- Bedding, T. R. 2011, ArXiv e-prints 1107.1723
- Bedding, T. R., Huber, D., Stello, D., et al. 2010, ApJLetters, 713, L176
- Bedding, T. R., Mosser, B., Huber, D., et al. 2011, Nature, 471, 608
- Belkacem, K., Goupil, M. J., Dupret, M. A., et al. 2011, A&A, 530, A142
- Borucki, W. J., Koch, D., Basri, G., et al. 2010, Science, 327, 977
- Carrier, F., De Ridder, J., Baudin, F., et al. 2010, A&A, 509, A73
- Christensen-Dalsgaard, J. 2011, ArXiv e-prints 1106.5946

- Corsaro, E., Stello, D., Huber, D., et al. 2012, *ApJ*, 757, 190
- De Ridder, J., Barban, C., Baudin, F., et al. 2009, *Nature*, 459, 398
- di Mauro, M. & al. 2013, these proceedings
- di Mauro, M. P., Cardini, D., Catanzaro, G., et al. 2011, *MNRAS*, 415, 3783
- Dziembowski, W. A. & Soszyński, I. 2010, *A&A*, 524, A88
- Eddington, A. S. 1917, *The Observatory*, 40, 290
- Frandsen, S., Carrier, F., Aerts, C., et al. 2002, *A&A*, 394, L5
- Hekker, S., Elsworth, Y., De Ridder, J., et al. 2011, *A&A*, 525, A131
- Hekker, S., Kallinger, T., Baudin, F., et al. 2009, *A&A*, 506, 465
- Huber, D., Bedding, T. R., Stello, D., et al. 2011, *ApJ*, 743, 143
- Huber, D., Bedding, T. R., Stello, D., et al. 2010, *ApJ*, 723, 1607
- Jiang, C., Jiang, B. W., Christensen-Dalsgaard, J., et al. 2011, *ApJ*, 742, 120
- Kallinger, T., Hekker, S., Mosser, B., et al. 2012, *A&A*, 541, A51
- Kallinger, T., Mosser, B., Hekker, S., et al. 2010, *A&A*, 522, A1
- Mathur, S., Hekker, S., Trampedach, R., et al. 2011, *ApJ*, 741, 119
- Michel, E., Baglin, A., Auvergne, M., et al. 2008, *Science*, 322, 558
- Miglio, A. & al. 2013, these proceedings
- Miglio, A., Montalbán, J., Baudin, F., et al. 2009, *A&A*, 503, L21
- Miglio, A., Montalbán, J., Carrier, F., et al. 2010, *A&A*, 520, L6
- Miglio, A., Morel, T., Barbieri, M., et al. 2012, in *European Physical Journal Web of Conferences*, Vol. 19, *European Physical Journal Web of Conferences*, 5012
- Montalbán, J., Miglio, A., Noels, A., et al. 2012, *Adiabatic Solar-Like Oscillations in Red Giant Stars*, ed. A. Miglio, J. Montalbán, & A. Noels, 23
- Mosser, B. 2010, *Astronomische Nachrichten*, 331, 944
- Mosser, B. & Appourchaux, T. 2009, *A&A*, 508, 877
- Mosser, B., Barban, C., Montalbán, J., et al. 2011a, *A&A*, 532, A86
- Mosser, B., Belkacem, K., Goupil, M., et al. 2011b, *A&A*, 525, L9
- Mosser, B., Belkacem, K., Goupil, M., et al. 2010, *A&A*, 517, A22
- Mosser, B., Elsworth, Y., Hekker, S., et al. 2012a, *A&A*, 537, A30
- Mosser, B., Goupil, M. J., Belkacem, K., et al. 2012b, *ArXiv e-prints* 1209.3336
- Mosser, B., Goupil, M. J., Belkacem, K., et al. 2012c, *A&A*, 540, A143
- Mosser, B., Michel, E., Belkacem, K., et al. 2013, submitted to *A&A*
- Provost, J., Mosser, B., & Berthomieu, G. 1993, *A&A*, 274, 595
- Roxburgh, I. W. 2009, *A&A*, 506, 435
- Samadi, R., Belkacem, K., Dupret, M.-A., et al. 2012, *A&A*, 543, A120
- Stello, D., Huber, D., Kallinger, T., et al. 2011, *ApJLetters*, 737, L10
- Tassoul, M. 1980, *ApJS*, 43, 469
- Unno, W., Osaki, Y., Ando, H., Saio, H., & Shibahashi, H. 1989, *Nonradial oscillations of stars*, ed. Unno, W., Osaki, Y., Ando, H., Saio, H., & Shibahashi, H. (Tokyo: University of Tokyo Press)
- White, T. R., Bedding, T. R., Stello, D., et al. 2011, *ApJLetters*, 742, L3